

## Supporting information

### Facile fabrication and characterization of rare-earth complexes based on Keggin-polyoxometalate with highly efficient activity for photocatalytic degradation of MO

Ying-Yu Li, <sup>†a</sup> Guan-Yu Jin, <sup>†a</sup> Zhi-Qiang Wang, <sup>†a</sup> Cong Hu, <sup>a</sup> Xue-Dong Wang, <sup>b</sup> Jian-Ming Liu, <sup>c</sup> Min Liu, <sup>d</sup> Hong-Liang Han, <sup>\*a</sup> Zhong-Feng Li<sup>\*a</sup> and Qiong-Hua Jin<sup>\*a,e,f</sup>

a. Department of Chemistry, Capital Normal University, Beijing 100048, China. E-mail: jinqh@cnu.edu.cn, jinqh204@163.com.

b. College of Resource Environment and Tourism, Capital Normal University, Beijing 100048, China.

c. School of Mathematical Sciences, Peking University, Beijing 100871, China.

d. Laboratory of Advanced Functional Materials, Ministry of Education, Faculty of Materials and Manufacturing, Beijing University of Technology, Beijing 100124, China.

e. State Key Laboratory of Elemento-Organic Chemistry, Nankai University, Tianjin 300071, China.

f. Key Laboratory of Advanced Energy Materials Chemistry (Ministry of Education), Nankai University, Tianjin 300071, China.

<sup>†</sup>Ying-Yu Li, Guan-Yu Jin and Zhi-Qiang Wang contributed equally to this work.

Electronic Supplementary Information (ESI) available: crystal structure information, IR spectra, etc. CCDC 2262909-2262914. For ESI and crystallographic data in CIF or other electronic format See DOI: 10.1039/x0xx00000x

#### Caption of Figure

**Fig. S1** (a)-(f) Micrographs of obtained crystals of complexes **1-6**.

**Fig. S2** (a) Formation of 2D structural plane by hydrogen bonding for complex **2**; (b)-(d) molecular stacking structure of complex **2**. (some hydrogen atoms are omitted)

**Fig. S3** (a) Formation of 2D structural plane by hydrogen bonding for complex **3**; (b)-(d) molecular stacking structure of complex **3**. (some hydrogen atoms are omitted)

**Fig. S4** (a) Formation of 2D structural plane by hydrogen bonding for complex **4**; (b)-(d) molecular stacking structure of complex **4**. (some hydrogen atoms are omitted)

**Fig. S5** (a) Formation of 2D structural plane by hydrogen bonding for complex **5**; (b)-(d) molecular stacking structure of complex **5**. (some hydrogen atoms are omitted)

**Fig. S6** (a) Formation of 2D structural plane by hydrogen bonding for complex **6**; (b)-(d) molecular stacking structure of complex **6**. (some hydrogen atoms are omitted)

**Fig. S7** The IR spectra for complex **1**.

**Fig. S8** The IR spectra for complex **2**.

**Fig. S9** The IR spectra for complex **3**.  
**Fig. S19** The IR spectra for complex **4**.  
**Fig. S11** The IR spectra for complex **5**.  
**Fig. S12** The IR spectra for complex **6**.  
**Fig. S13** Powder X-ray diffraction of complex **1**.  
**Fig. S14** Powder X-ray diffraction of complex **2**.  
**Fig. S15** Powder X-ray diffraction of complex **3**.  
**Fig. S16** Powder X-ray diffraction of complex **4**.  
**Fig. S17** Powder X-ray diffraction of complex **5**.  
**Fig. S18** Powder X-ray diffraction of complex **6**.  
**Fig. S19** Thermogravimetric curves of complexes **1-6**.  
**Fig. S20** Scanning electron micrographs of complexes **1-6**.  
**Fig. S21** EDS mapping of  $[\text{DyL}_3(\text{H}_2\text{O})]\text{PW}_{12}\text{O}_{40}\cdot\text{CH}_3\text{CN}@PVDF$ .  
**Fig. S22** Selective adsorption properties of complex **1**.  
**Fig. S23** Solid UV-Vis diffuse reflectance spectrum of K-M function vs  $E_g$  for complexes **1-6**.  
**Fig. S24** Comparison of PXRD before and after catalysis of complex **1**.  
**Fig. S25** Degradation efficiency of complex **1**@PVDF in different inhibitors.  
**Fig. S26** Terahertz spectra of complexes **1-6**.

### **Caption of Table**

**Table S1** Selected bond lengths( $\text{\AA}$ ) and bond angles( $^\circ$ ) for complexes **1-6**.  
**Table S2** Weak interactions in the stacking structure of complex **1**.  
**Table S3** Weak interactions in the stacking structure of complex **2**.  
**Table S4** Weak interactions in the stacking structure of complex **3**.  
**Table S5** Weak interactions in the stacking structure of complex **4**.  
**Table S6** Weak interactions in the stacking structure of complex **5**.  
**Table S7** Weak interactions in the stacking structure of complex **6**.  
**Table S8** Efficiency of methyl orange degradation by complexes **1-6**.  
**Table S9** Comparison of the photocatalytic activities of reported polyacid-based complexes.

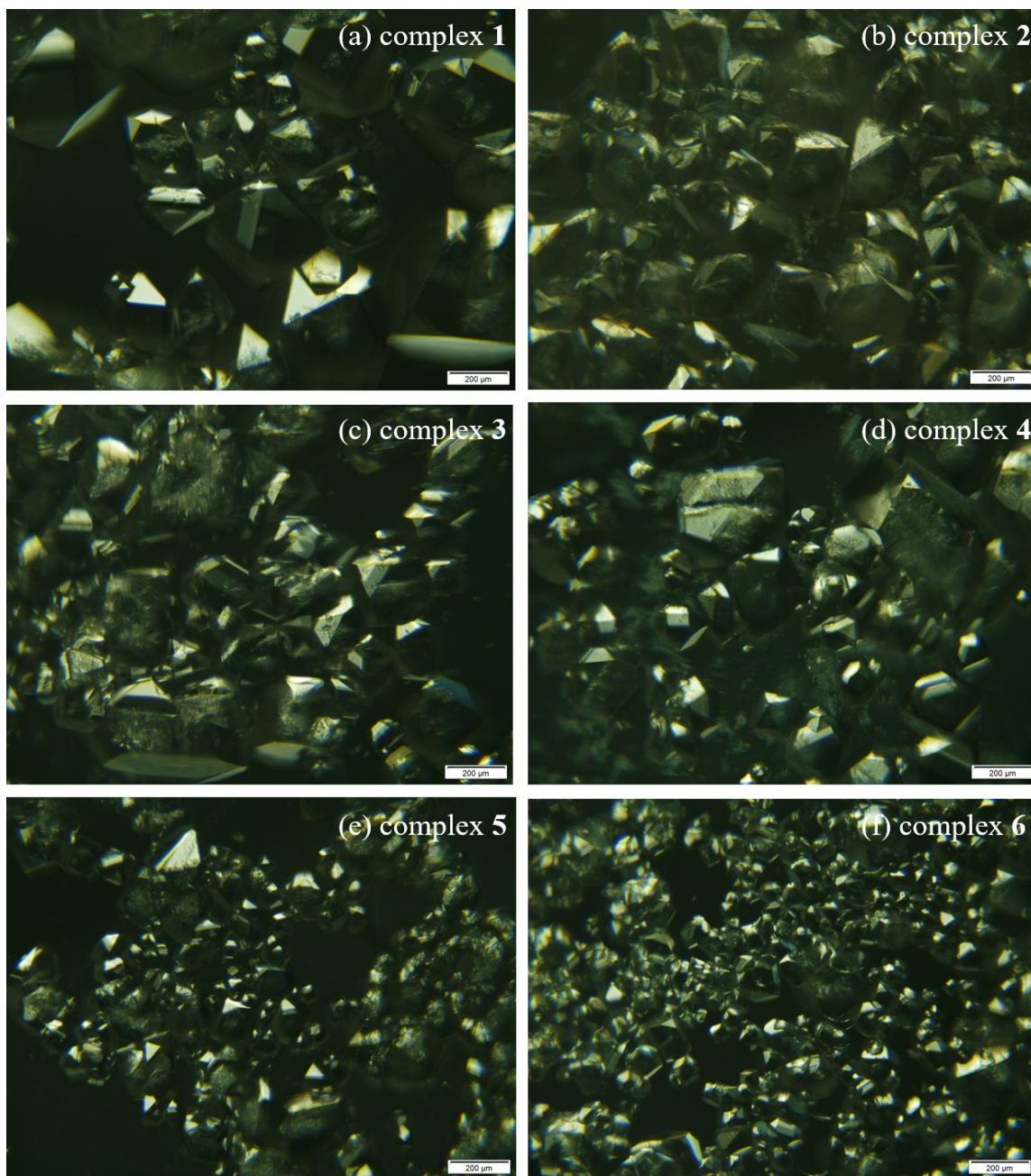


**Fig. S1** (a)-(f) Micrographs of obtained crystals of complexes 1-6.

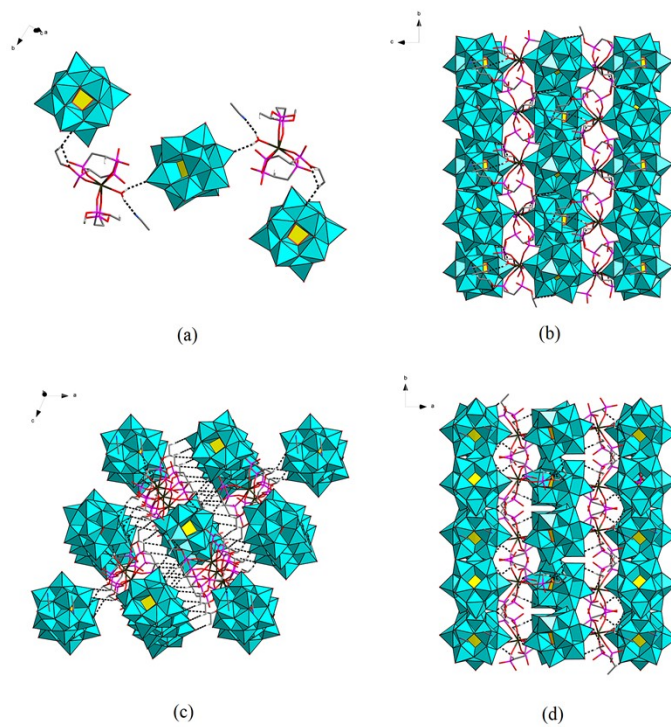


**Fig. S2** (a) Formation of 2D structural plane by hydrogen bonding for complex **2**; (b)-(d) molecular stacking structure of complex **2**. (some hydrogen atoms are omitted)

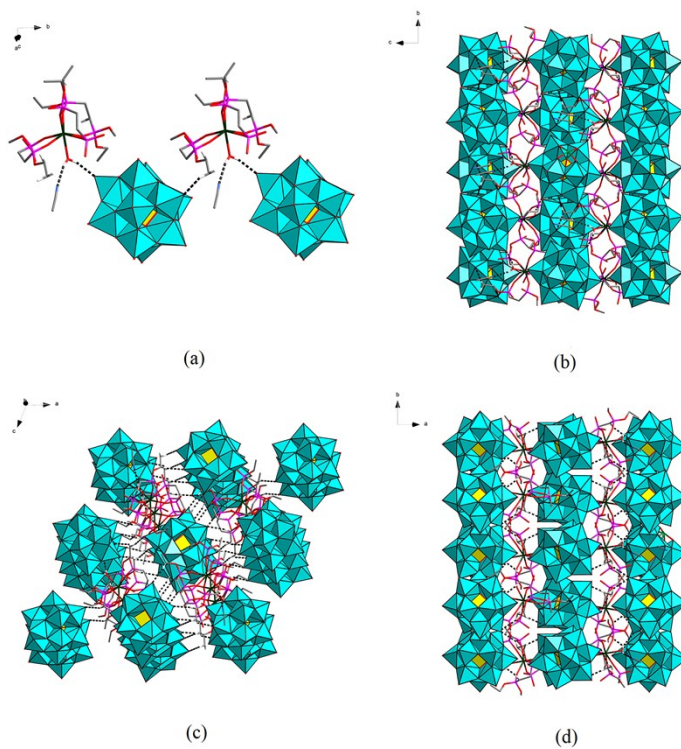


**Fig. S3** (a) Formation of 2D structural plane by hydrogen bonding for complex **3**; (b)-(d) molecular stacking structure of complex **3**. (some hydrogen atoms are omitted)

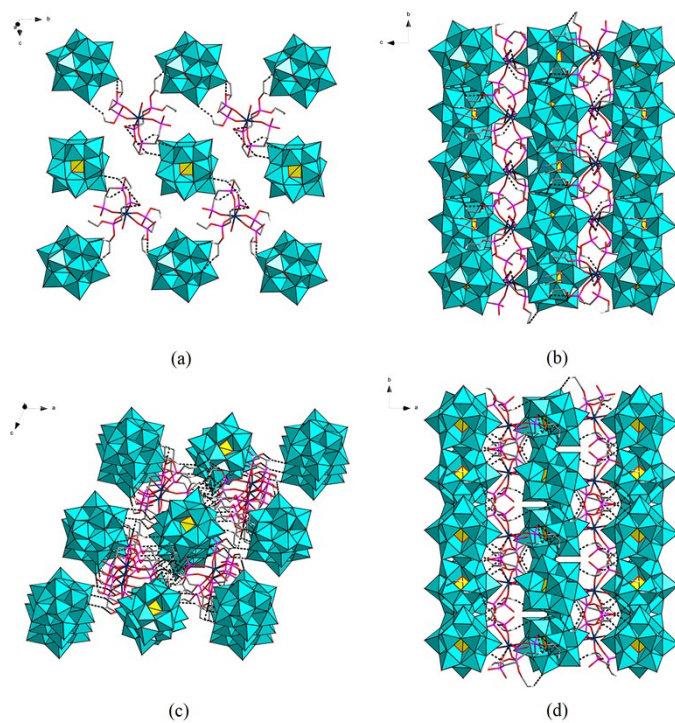


**Fig. S4** (a) Formation of 2D structural plane by hydrogen bonding for complex 4; (b)-(d) molecular stacking structure of complex 4. (some hydrogen atoms are omitted)

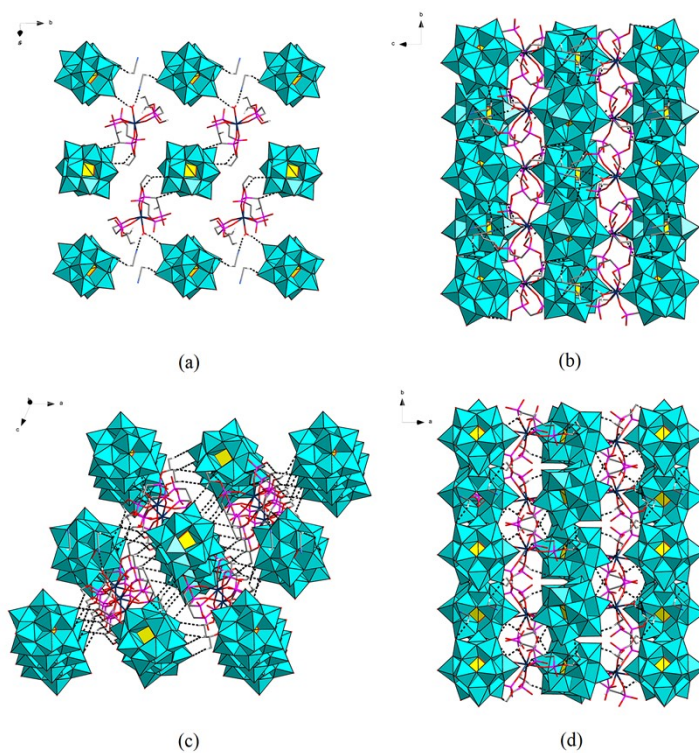


**Fig. S5** (a) Formation of 2D structural plane by hydrogen bonding for complex 5; (b)-(d) molecular stacking structure of complex 5. (some hydrogen atoms are omitted)

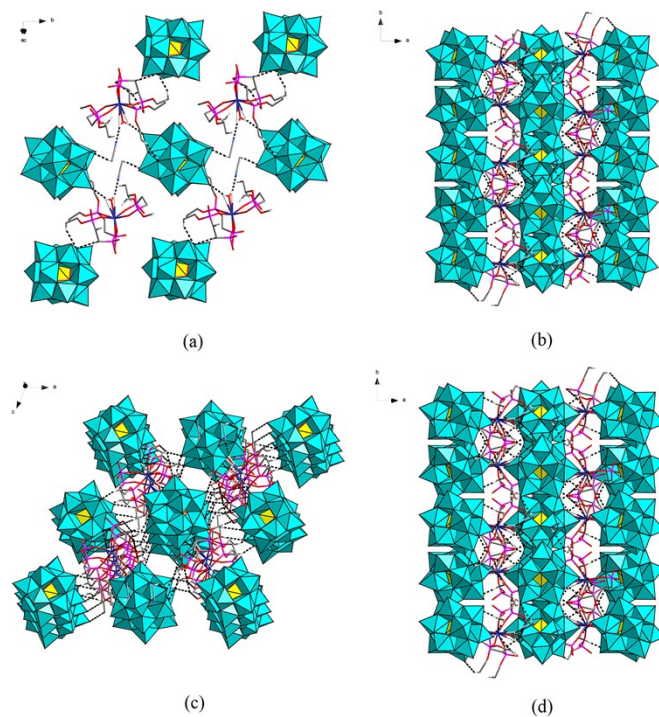


**Fig. S6** (a) Formation of 2D structural plane by hydrogen bonding for complex 6; (b)-(d) molecular stacking structure of complex 6. (some hydrogen atoms are omitted)

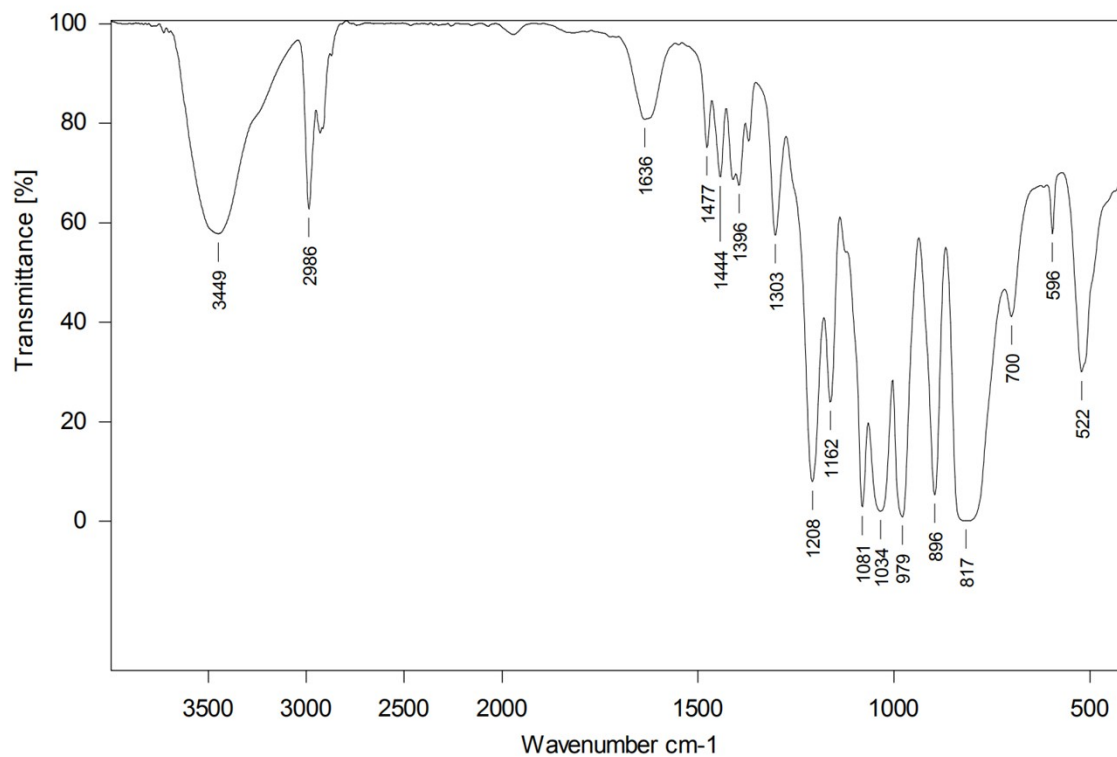


**Fig. S7** The IR spectra for complex 1.

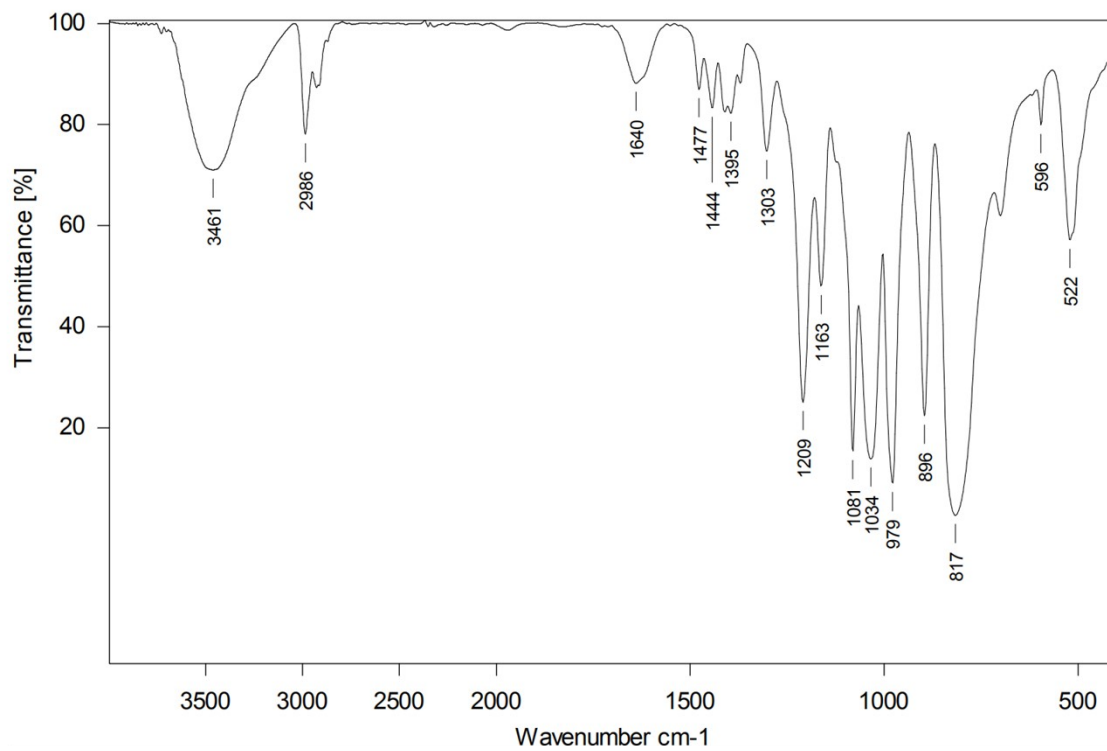


**Fig. S8** The IR spectra for complex 2.

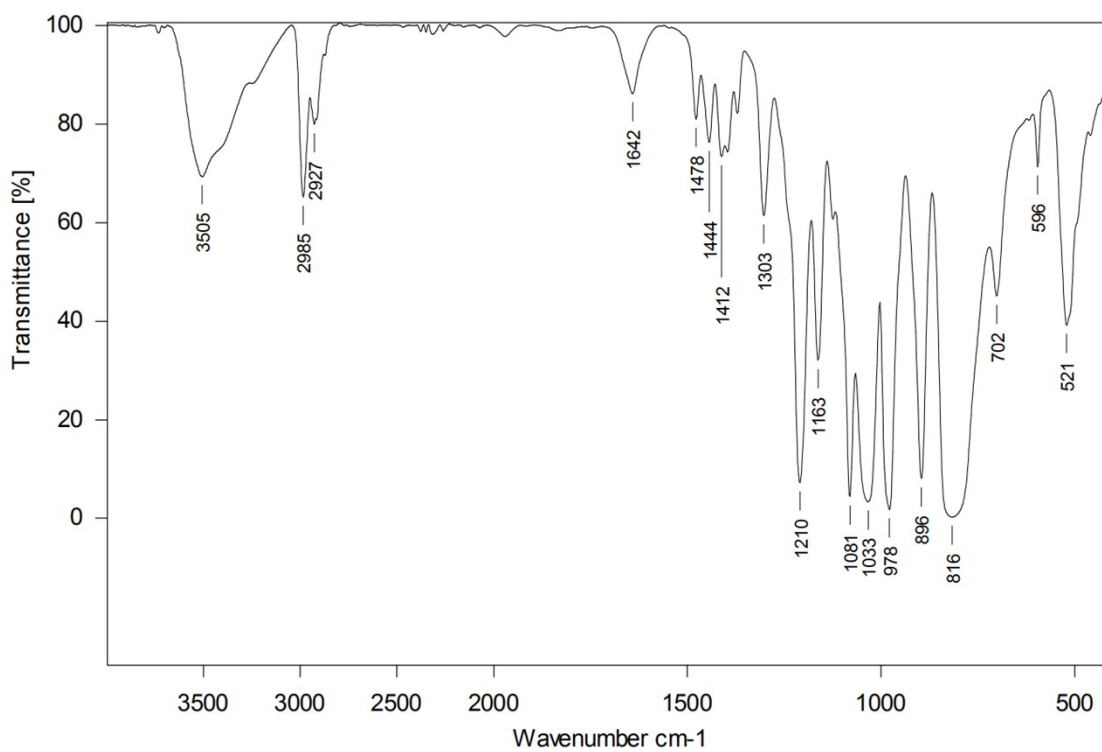


**Fig. S9** The IR spectra for complex 3.

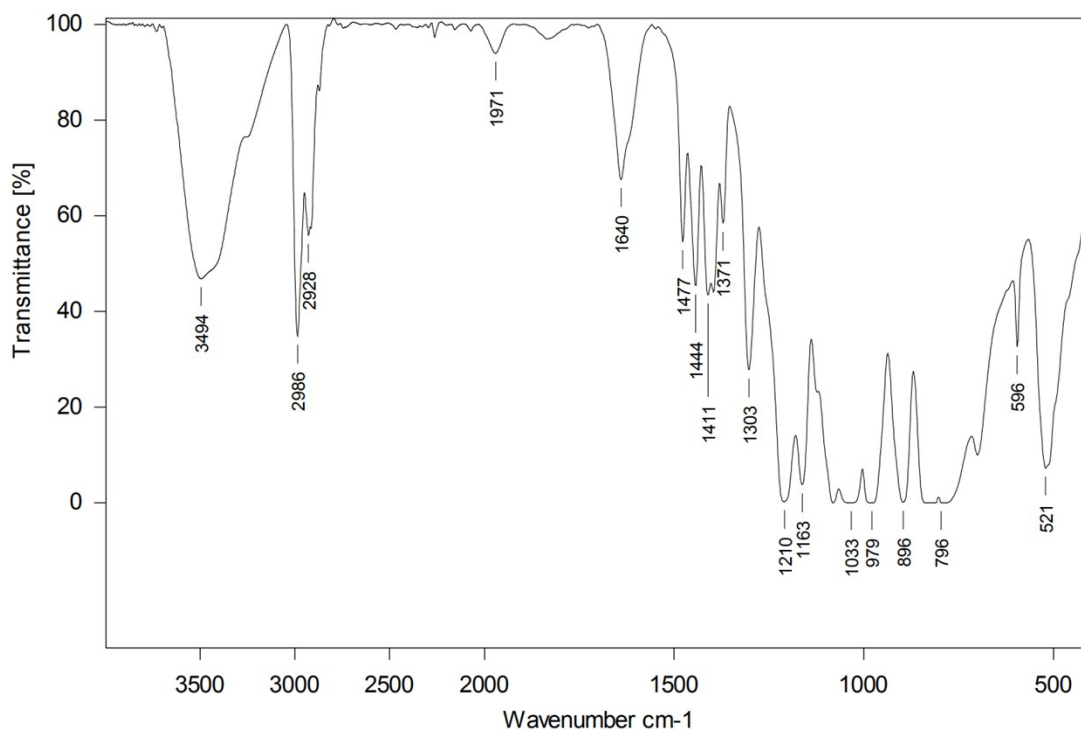


**Fig. S10** The IR spectra for complex 4.

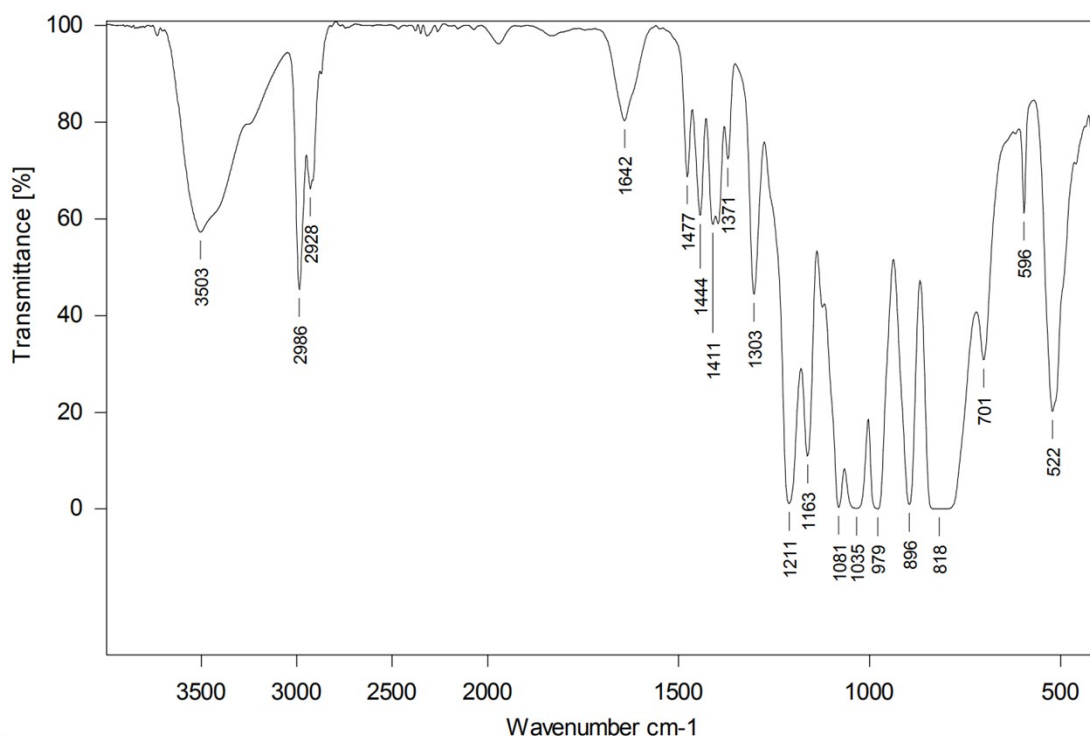


**Fig. S11** The IR spectra for complex 5.



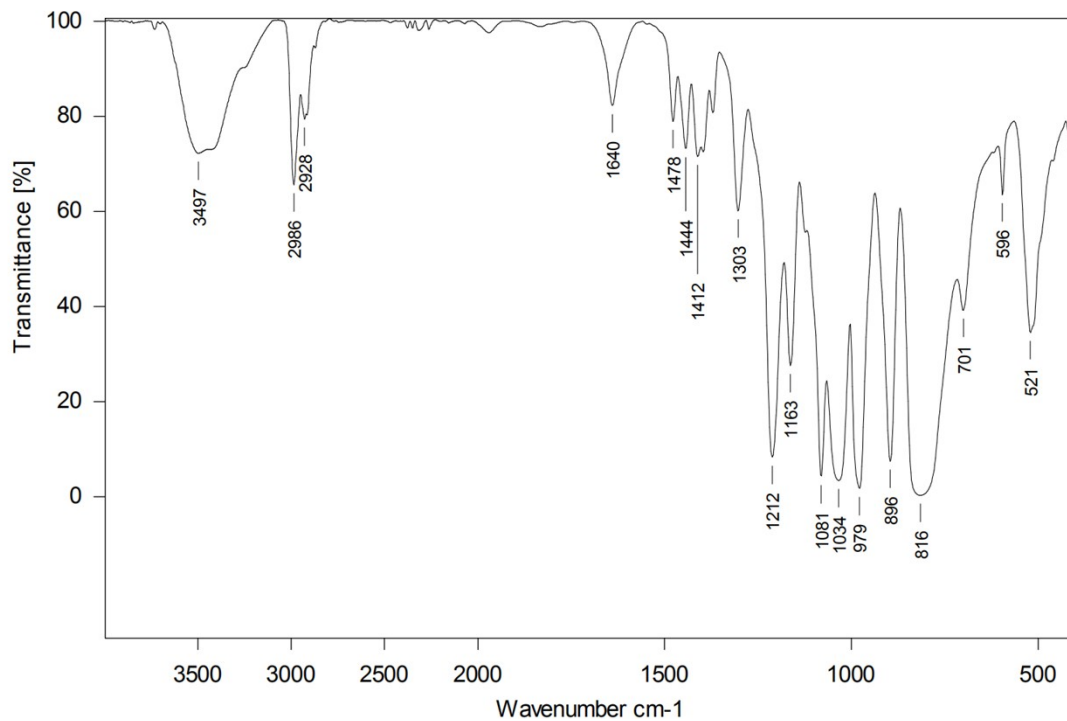


**Fig. S12** The IR spectra for complex 6.

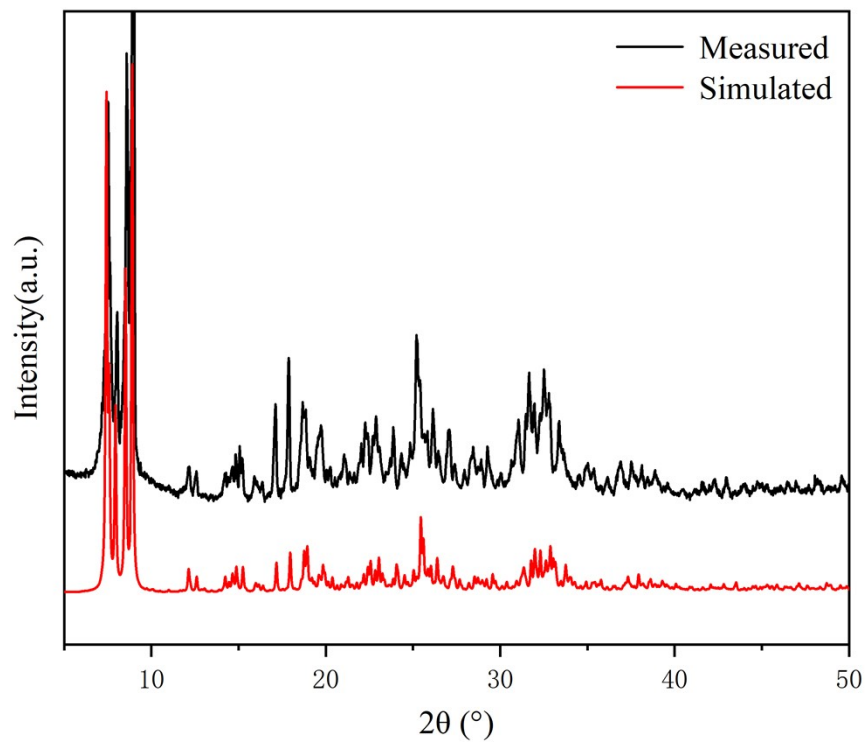


**Fig. S13** Powder X-ray diffraction of complex 1.

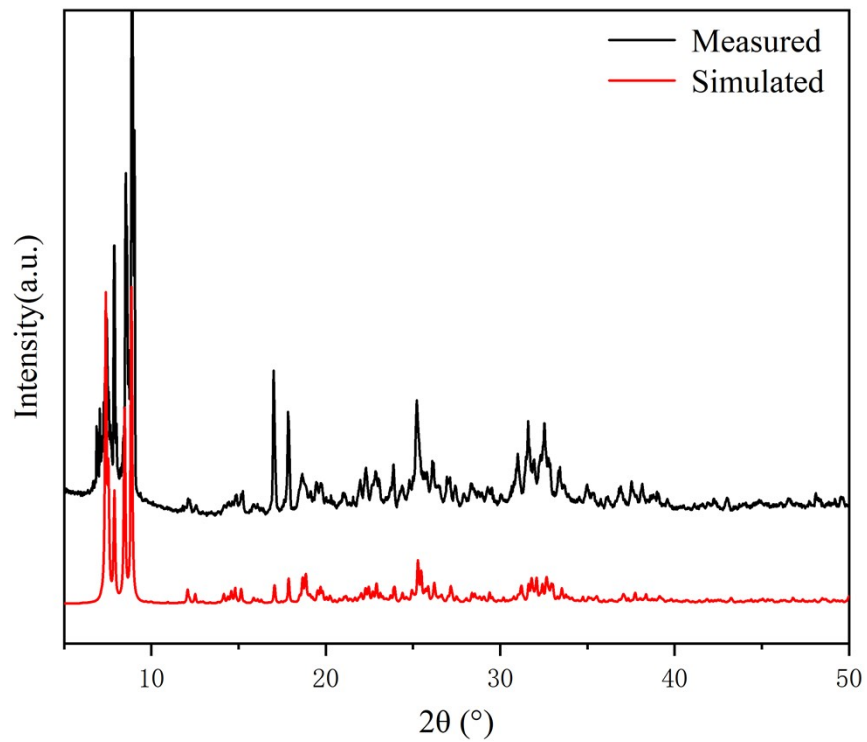


**Fig. S14** Powder X-ray diffraction of complex **2**.

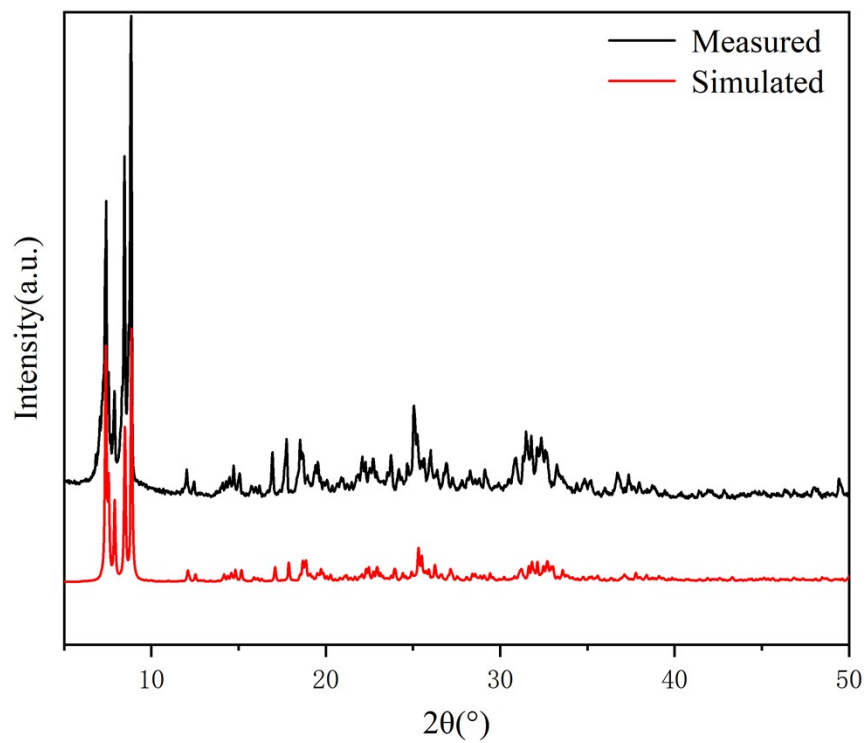


**Fig. S15** Powder X-ray diffraction of complex **3**.

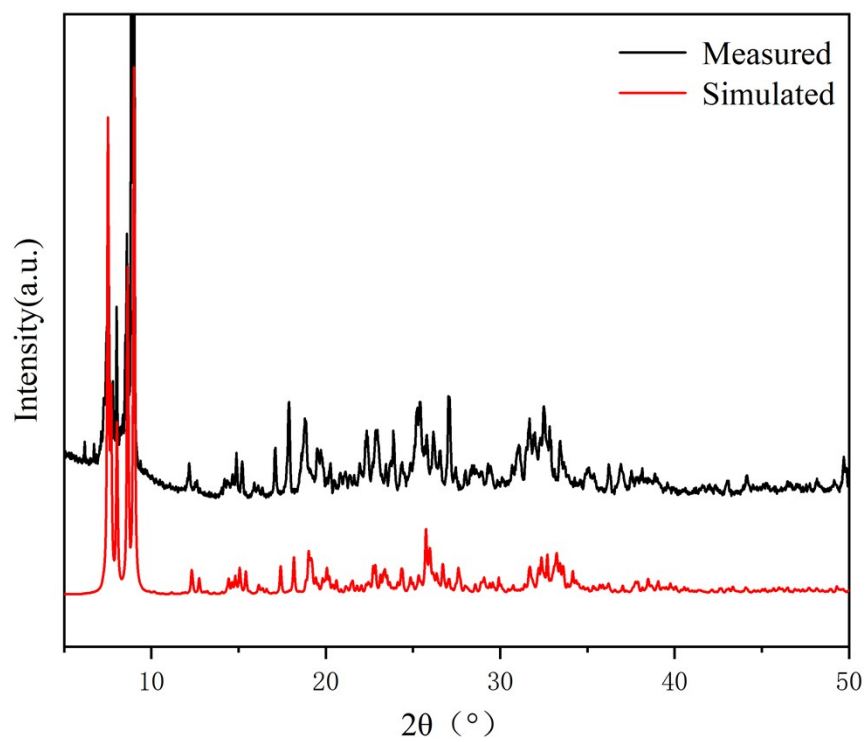


**Fig. S16** Powder X-ray diffraction of complex 4.

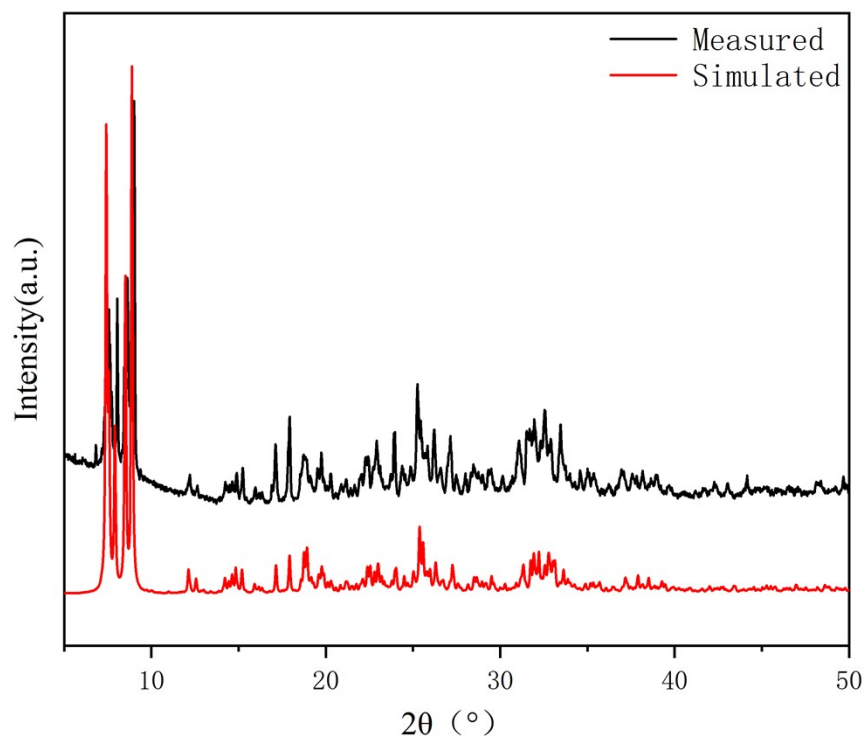


**Fig. S17** Powder X-ray diffraction of complex 5.

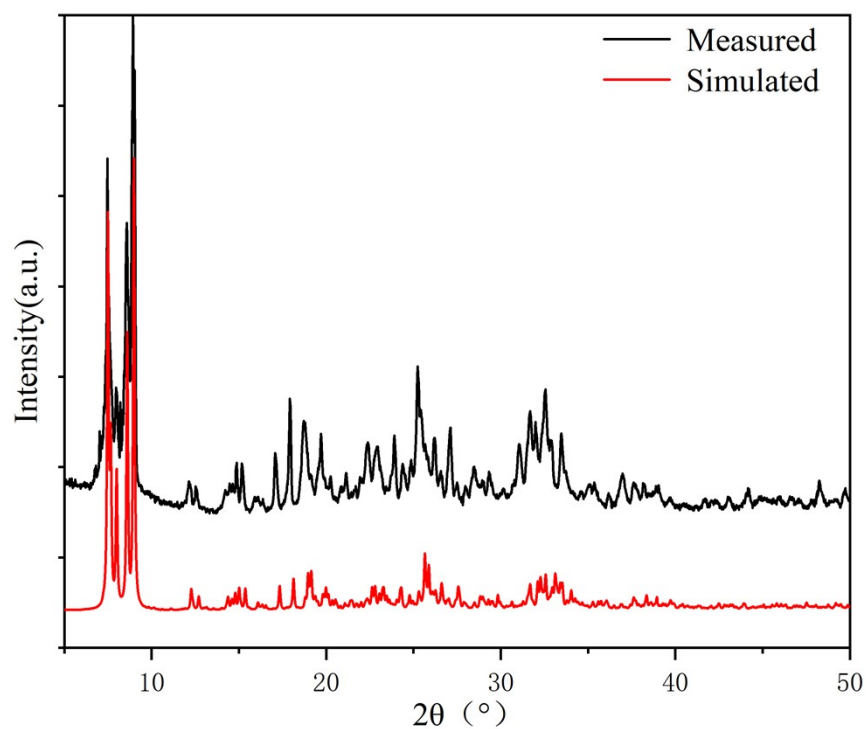


**Fig. S18** Powder X-ray diffraction of complex **6**.

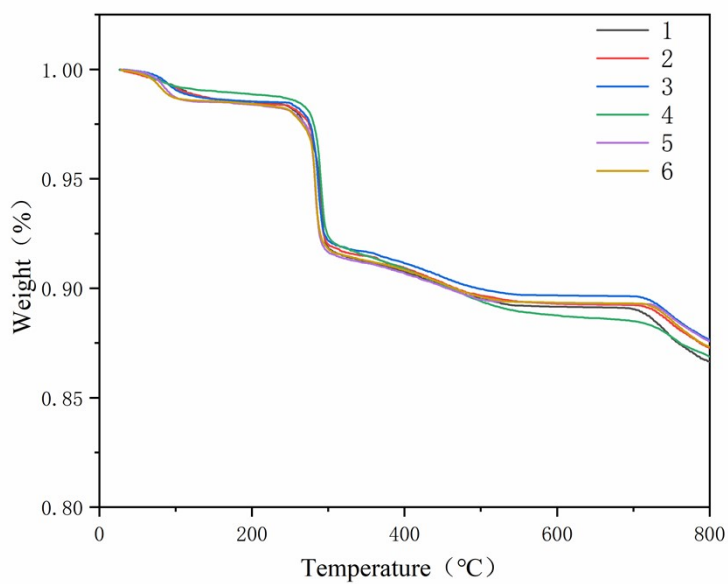


**Fig. S19** Thermogravimetric curves of complexes **1-6**.

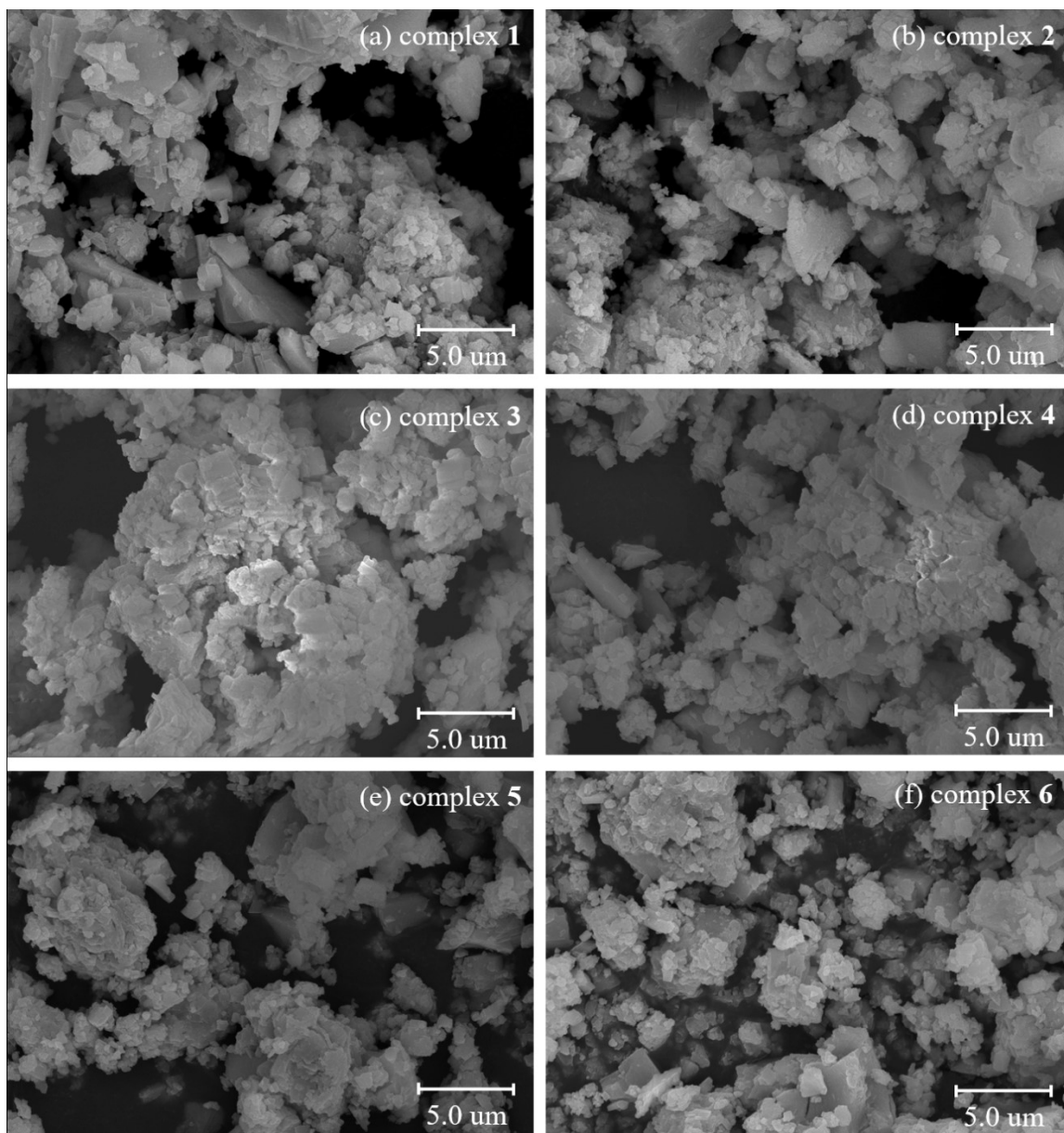


**Fig. S20** Scanning electron micrographs of complexes 1-6.

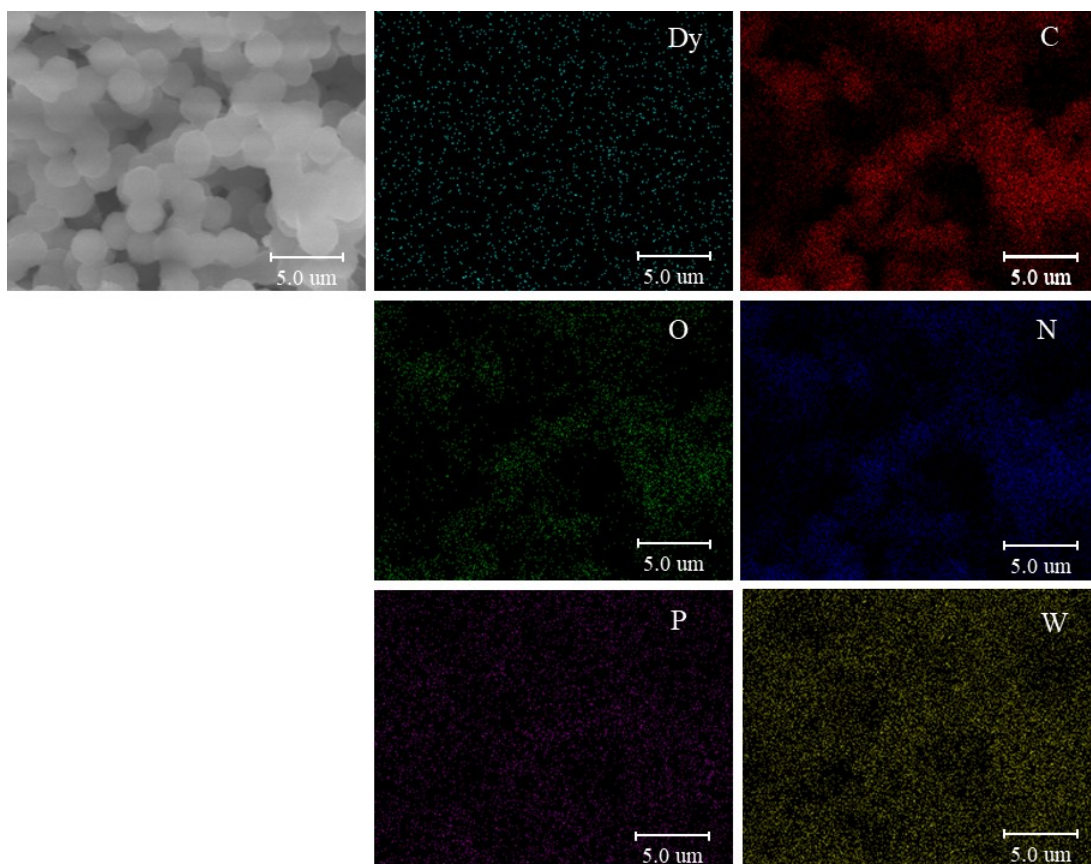


**Fig. S21** EDS mapping of  $[\text{DyL}_3(\text{H}_2\text{O})]\text{PW}_{12}\text{O}_{40}\cdot\text{CH}_3\text{CN}@PVDF$ .

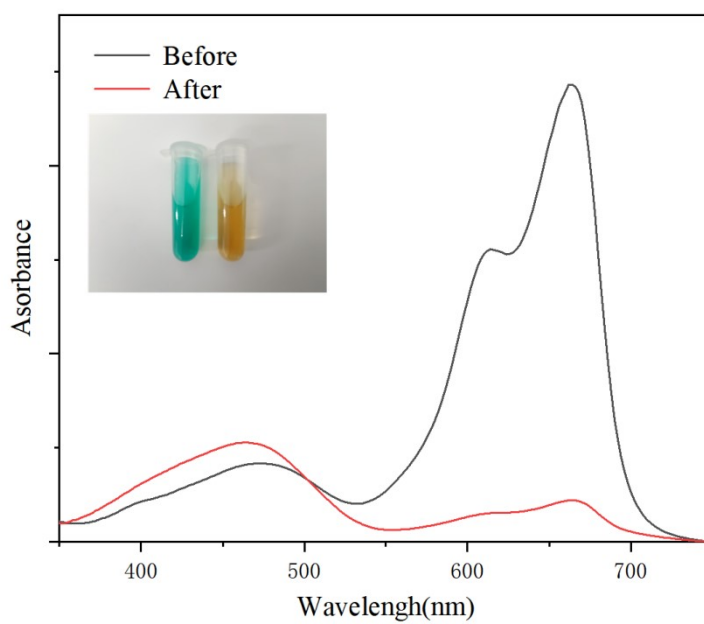


**Fig. S22** Selective adsorption properties of complex **1**.

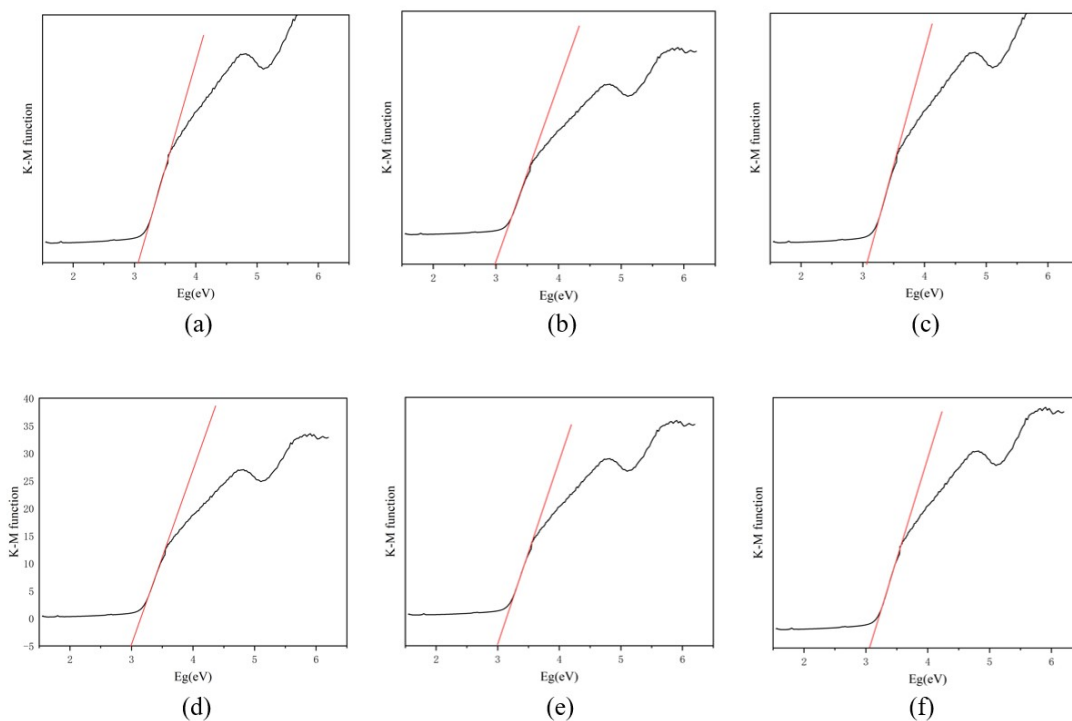


**Fig. S23** Solid UV-Vis diffuse reflectance spectrum of K-M function vs  $E_g$  for complexes **1-6**.

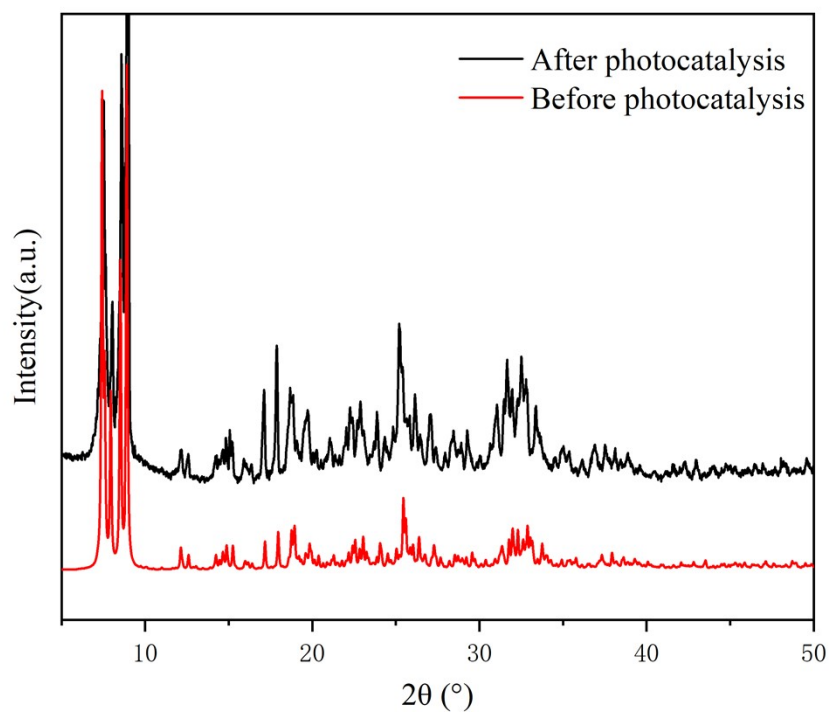


**Fig. S24** Comparison of PXRD before and after catalysis of complex **1**.

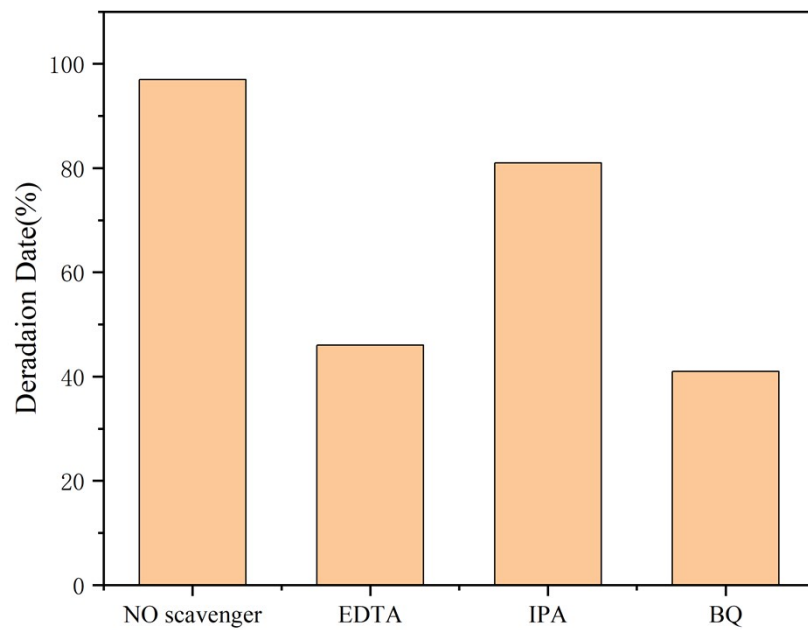


**Fig. S25** Degradation efficiency of complex 1@PVDF in different inhibitors.

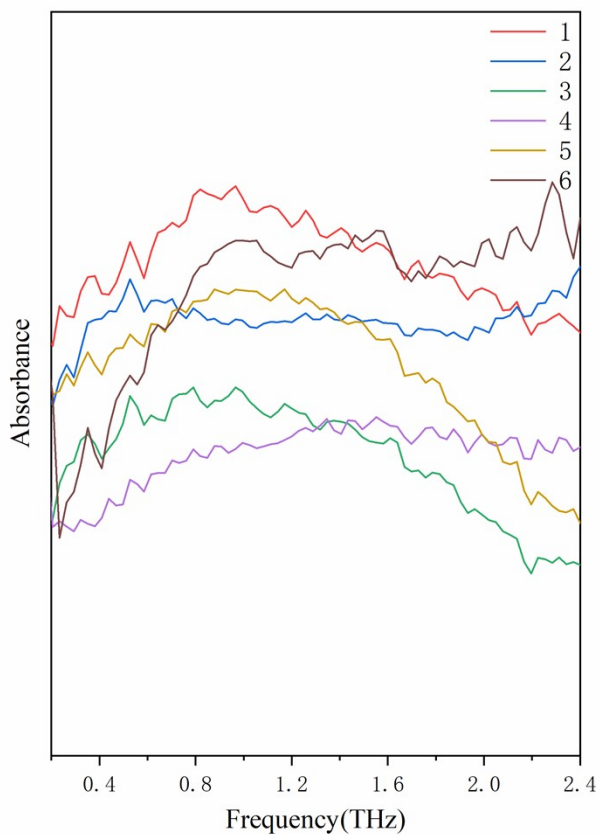


**Fig. S26** Terahertz spectra of complexes 1-6.



**Table S1** Selected bond lengths(Å) and bond angles(°) for complexes **1-6**.

Complex 1					
Dy(1)–O(16)	2.24(3)	Dy(1)–O(7)	2.25(3)	Dy(1)–O(10)	2.27(3)
Dy(1)–O(13)	2.27(3)	Dy(1)–O(1)	2.28(3)	Dy(1)–O(4)	2.33(3)
Dy(1)–O(19)	2.41(3)				
O(1)–Dy(1)–O(4)	76.4(10)	O(7)–Dy(1)–O(10)	77.5(10)	O(13)–Dy(1)–O(16)	79.1(11)
Complex 2					
Ho(1)–O(16)	2.2233(17)	Ho(1)–O(7)	2.250(16)	Ho(1)–O(4)	2.291(16)
Ho(1)–O(13)	2.292(16)	Ho(1)–O(1)	2.297(17)	Ho(1)–O(10)	2.298(15)
Ho(1)–O(19)	2.370(16)				
O(1)–Ho(1)–O(4)	75.9(6)	O(7)–Ho(1)– O(10)	77.5(6)	O(13)–Ho(1)–O(16)	78.9(6)
Complex 3					
Er(1)–O(1)	2.227(15)	Er(1)–O(4)	2.270(16)	Er(1)–O(7)	2.249(15)
Er(1)–O(10)	2.260(15)	Er(1)–O(13)	2.249(15)	Er(1)–O(16)	2.227(17)
Er(1)–O(19)	2.378(14)				
O(1)–Er(1)–O(4)	76.4(5)	O(7)–Er(1)–O(10)	78.8(5)	O(13)–Er(1)–O(16)	78.6(6)
Complex 4					
Tm(1)–O(1)	2.23(2)	Tm(1)–O(4)	2.23(2)	Tm(1)–O(7)	2.18(2)
Tm(1)–O(10)	2.20(2)	Tm(1)–O(13)	2.25(2)	Tm(1)–O(16)	2.18(2)
Tm(1)–O(19)	2.29(2)				
O(1)–Tm(1)–O(4)	76.2(8)	O(7)–Tm(1)– O(10)	77.9(8)	O(13)–Tm(1)–O(16)	80.6(9)
Complex 5					
Yb(1)–O(1)	2.247(16)	Yb(1)–O(4)	2.261(13)	Yb(1)–O(7)	2.244(13)
Yb(1)–O(10)	2.283(14)	Yb(1)–O(13)	2.290(15)	Yb(1)–O(16)	2.182(15)
Yb(1)–O(19)	2.377(14)				
O(1)–Yb(1)–O(4)	75.8(5)	O(7)–Yb(1)–O(10)	78.0(5)	O(13)–Yb(1)–O(16)	78.7(6)
Complex 6					

Lu(1)–O(1)	2.200(17)	Lu(1)–O(4)	2.232(15)	Lu(1)–O(7)	2.172(14)
Lu(1)–O(10)	2.200(15)	Lu(1)–O(13)	2.216(15)	Lu(1)–O(16)	2.218(15)
Lu(1)–O(19)	2.297(17)				
O(1)–Lu(1)–O(4)	75.5(6)	O(7)–Lu(1)–O(10)	78.2(6)	O(13)–Lu(1)–O(16)	79.0(6)

**Table S2** Weak interactions in the stacking structure of complex **1**.

Intermolecular hydrogen bonds in the stacking structure of complex **1**

Donor-H...Acceptor	D-H (Å)	H...A (Å)	D-H...A (°)
O(19)-H(19E)...N(1)	0.86	2.12	162
O(19)-H(19F)...O(28)	0.86	2.03	166
C(7)-H(7A)...O(39)	0.97	2.58	141
C(10)-H(10C)...O(58)	0.96	2.53	160
C(19)-H(19A)...O(53)	0.97	2.57	128
C(20)-H(20B)...O(2)	0.96	2.58	153
C(23)-H(23A)...O(57)	0.97	2.59	159
C(24)-H(24C)...O(33)	0.95	2.17	148
C(27)-H(27A)...O(39)	0.96	2.56	142
C(27)-H(27B)...O(33)	0.98	2.57	157
C(32)-H(32A)...O(33)	0.96	2.4	146

Intramolecular hydrogen bonding in the stacking structure of complex **1**

Donor-H...Acceptor	D-H (Å)	H...A (Å)	D-H...A (°)
C(7)-H(7B)...O(6)	0.97	2.45	141
C(13)-H(13A)...O(9)	0.96	2.60	103
C(17)-H(17A)...O(15)	0.97	2.43	163
C(25)-H(25A)...O(14)	0.97	2.55	101

C(29)-H(29A)···O(16)	0.97	2.53	110
----------------------	------	------	-----

**Table S3** Weak interactions in the stacking structure of complex **2**.

Intermolecular hydrogen bonds in the stacking structure of complex **2**

Donor-H···Acceptor	D-H (Å)	H···A (Å)	D-H···A (°)
O(19)-H(19E)···N(1)	0.87	2.1	164
O(19)-H(19F)···O(28)	0.86	2.11	165
C(2)-H(2B)···O(36)	0.97	2.48	162
C(12)-H(12B)···O(53)	0.97	2.58	160
C(19)-H(19A)···O(53)	0.97	2.34	156
C(20)-H(20A)···O(56)	0.96	2.5	160
C(23)-H(23A)···O(57)	0.97	2.56	171
C(24)-H(24B)···O(63)	0.96	2.54	159
C(27)-H(27B)···O(33)	0.97	2.49	165

Intramolecular hydrogen bonding in the stacking structure of complex **2**

Donor-H···Acceptor	D-H (Å)	H···A (Å)	D-H···A (°)
C(3)-H(3B)···O(58)	0.97	2.58	100
C(15)-H(15A)···O(8)	0.97	2.38	106
C(25)-H(25A)···O(14)	0.97	2.55	101

**Table S4** Weak interactions in the stacking structure of complex **3**.

Intermolecular hydrogen bonds in the stacking structure of complex **3**

Donor-H···Acceptor	D-H (Å)	H···A (Å)	D-H···A (°)
O(19)-H(19E)···N(1)	0.86	2.11	165
O(19)-H(19F)···O(28)	0.86	2.1	164

C(2)-H(2B)···O(36)	0.97	2.49	162
C(19)-H(19A)···O(53)	0.97	2.36	161
C(23)-H(23A)···O(57)	0.97	2.57	173
C(24)-H(24A)···O(33)	0.96	2.53	125
C(24)-H(24B)···O(63)	0.96	2.53	156

Intramolecular hydrogen bonding in the stacking structure of complex **3**

Donor-H···Acceptor	D–H (Å)	H···A (Å)	D–H···A (°)
C(3)-H(3B)···O(58)	0.97	2.58	130
C(5)-H(5B)···O(17)	0.97	2.56	129
C(25)-H(25A)···O(14)	0.97	2.57	102

**Table S5** Weak interactions in the stacking structure of complex **4**.

Intermolecular hydrogen bonds in the stacking structure of complex **4**

Donor-H···Acceptor	D-H (Å)	H···A (Å)	D-H···A (°)
O(19)-H(19E)···N(1)	0.85	2.14	163
O(19)-H(19F)···O(28)	0.85	2.09	163
C(1)-H(1B)···O(58)	0.97	2.56	143
C(2)-H(2B)···O(36)	0.97	2.42	159
C(12)-H(12B)···O(53)	0.97	2.57	158
C(13)-H(13A)···O(27)	0.97	2.58	138
C(14)-H(14B)···O(30)	0.96	2.52	169
C(16)-H(16B)···O(50)	0.96	2.51	141
C(19)-H(19A)···O(53)	0.97	2.21	150
C(20)-H(20A)···O(56)	0.96	2.59	140
C(23)-H(23A)···O(57)	0.97	2.56	154

C(24)-H(24C)···O(33)	0.95	2.25	168
C(27)-H(27A)···O(39)	0.97	2.38	140
C(32)-H(32C)···O(33)	0.96	2.45	152

Intramolecular hydrogen bonding in the stacking structure of complex **4**

Donor-H···Acceptor	D–H (Å)	H···A (Å)	D–H···A (°)
C(2)-H(2B)···O(3)	0.97	2.58	112
C(3)-H(3B)···O(1)	0.97	2.47	101
C(3)-H(3B)···O(12)	0.97	2.50	112
C(5)-H(5A)···O(17)	0.97	2.59	112
C(17)-H(17A)···O(15)	0.97	2.47	117
C(22)-H(22A)···O(51)	0.97	2.56	104
C(25)-H(25A)···O(14)	0.97	2.57	100

**Table S6** Weak interactions in the stacking structure of complex **5**.

Intermolecular hydrogen bonds in the stacking structure of complex **5**

Donor-H···Acceptor	D–H (Å)	H···A (Å)	D–H···A (°)
O(19)-H(19E)···N(1)	0.86	2.06	163
O(19)-H(19F)···O(28)	0.86	2.09	165
C(1)-H(1B)···O(58)	0.97	2.6	148
C(2)-H(2B)···O(36)	0.97	2.48	161
C(19)-H(19A)···O(53)	0.97	2.39	154
C(20)-H(20A)···O(56)	0.96	2.46	156
C(23)-H(23A)···O(57)	0.97	2.49	161
C(24)-H(24B)···O(63)	0.96	2.49	170
C(27)-H(27B)···O(33)	0.97	2.57	159
C(29)-H(29A)···O(36)	0.97	2.58	137

C(32)-H(32C)···O(33)	0.96	2.49	156
----------------------	------	------	-----

Intramolecular hydrogen bonding in the stacking structure of complex **5**

Donor-H···Acceptor	D–H (Å)	H···A (Å)	D–H···A (°)
C(2)-H(2B)···O(3)	0.97	2.58	111
C(3)-H(3B)···O(1)	0.97	2.58	102
C(3)-H(3B)···O(12)	0.97	2.51	112
C(17)-H(17A)···O(15)	0.97	2.52	160
C(23)-H(23B)···O(13)	0.97	2.47	111

**Table S7** Weak interactions in the stacking structure of complex **6**.

Intermolecular hydrogen bonds in the stacking structure of complex **6**

Donor-H···Acceptor	D-H (Å)	H···A (Å)	D-H···A (°)
O(19)-H(19E)···N(1)	0.85	2.1	162
O(19)-H(19F)···O(28)	0.85	2.11	164
C(1)-H(1B)···O(58)	0.97	2.51	147
C(2)-H(2B)···O(36)	0.97	2.4	161
C(10)-H(10C)···O(58)	0.96	2.59	147
C(14)-H(14B)···O(30)	0.96	2.54	162
C(16)-H(16B)···O(50)	0.96	2.6	142
C(19)-H(19A)···O(53)	0.97	2.3	156
C(23)-H(23A)···O(57)	0.97	2.53	177
C(24)-H(24B)···O(63)	0.96	2.35	176
C(27)-H(27B)···O(33)	0.97	2.55	156
C(29)-H(29A)···O(36)	0.97	2.43	133
C(32)-H(32A)···O(33)	0.96	2.54	143

Intramolecular hydrogen bonding in the stacking structure of complex **6**

Donor-H...Acceptor	D-H (Å)	H...A (Å)	D-H...A (°)
C(2)-H(2B)...O(3)	0.97	2.59	111
C(3)-H(3B)...O(12)	0.97	2.54	129
C(5)-H(5B)...O(17)	0.97	2.53	121
C(17)-H(17A)...O(15)	0.97	2.44	160
C(25)-H(25A)...O(14)	0.97	2.56	100

**Table S8** Efficiency of methyl orange degradation by complexes **1-6**.

	0min	3min	6min	9min	12min	15min
Complex <b>1</b>	0%	40.27%	70.35%	92.35%	95.48%	95.78%
Complex <b>2</b>	0%	22.51%	64.33%	92.53%	96.35%	97.41%
Complex <b>3</b>	0%	33.45%	70.32%	91.58%	95.06%	96.38%
Complex <b>4</b>	0%	34.05%	66.22%	86.93%	94.71%	95.84%
Complex <b>5</b>	0%	37.27%	65.28%	87.34%	94.62%	95.32%
Complex <b>6</b>	0%	26.75%	70.17%	87.07%	94.45%	95.02%

**Table S9** Comparison of the photocatalytic activities of reported polyacid-based complexes.

Catalysts	Light source	Degradation rate	Stability (cycle)	Ref.
Pt/H <sub>3</sub> PMo <sub>12</sub> O <sub>40</sub> /TiO <sub>2</sub>	300 W Xe lamp	82.56% in 180 min	5	1
TiO <sub>2</sub> /POM/Fe <sub>3</sub> O <sub>4</sub> @SiO <sub>2</sub>	300 W Hg lamp UV	97.32% in 100 min	1	2
H <sub>3</sub> PW <sub>12</sub> O <sub>40</sub> /SiO <sub>2</sub>	500 W Xe lamp	98.3% in 120 min	5	3
[{Ag <sub>5</sub> (pz) <sub>7</sub> }{AlW <sub>12</sub> O <sub>40</sub> }]·4H <sub>2</sub> O	125 W Hg lamp UV	90.33% in 175 min	1	4
Na(BiHEDTA·2H <sub>2</sub> O) <sub>3</sub> (PW <sub>12</sub> O <sub>40</sub> )·2H <sub>2</sub> O	300 W Xe lamp	96% in 80 min	5	5

$\text{Li}_4(\text{H}_2\text{O})_6[(\text{H}_2\text{V}_6\text{O}_{18})\cdot(\text{Me}_{10}\text{CB}[5]@\text{H}_2\text{O})_2]\cdot 14\text{H}_2\text{O}$	500W Xe lamp	75% in 180 min	5	6
$[\text{Cu}_4(\text{OH})_3\text{Cl}(\text{H}_2\text{O})_3(4\text{-bpo})_3](\text{SiW}_{12}\text{O}_{40})\cdot 5\text{H}_2\text{O}$	500 W Xe lamp	68.6% in 180 min	1	7
$\text{H}_9\text{Na}_3[\text{WZn}_3(\text{H}_2\text{O})_2(\text{ZnW}_9\text{O}_{34})_2]\cdot 24\text{H}_2\text{O}$	400W Hg lamp UV	99% in 7 min	1	8
$\text{Cu}_2(\text{L}_1)_3(\text{H}_2\text{O})_2(\text{Mo}_4\text{O}_{13})_2$	200 W Hg lamp UV	56% in 90 min	5	9
$\text{H}_3\text{PW}_{12}\text{O}_{40}/\text{Ag}_3\text{PO}_4$ Powder	300 Xe lamp	99% in 6 min	4	10
$\text{H}_3\text{PW}_{12}\text{O}_{40}/\text{Ag}_3\text{PO}_4@$ PVDF-F127	300 Xe lamp	75% in 60 min	4	11
$[\text{DyL}_3(\text{H}_2\text{O})]\text{PW}_{12}\text{O}_{40}\cdot\text{CH}_3\text{CN}$	400 W Hg lamp UV	95.8% in 15min	4	This work
$[\text{DyL}_3(\text{H}_2\text{O})]\text{PW}_{12}\text{O}_{40}\cdot\text{CH}_3\text{CN}@$ PVDF	400 W Hg lamp UV	97.4% in 50 min	4	This work

## References

- 1 H.-F. Shi, T.-T. Zhao, Z. Yue, H.-Q. Tan, W.-H. Shen, W.-D. Wang, Y.-G. Li and E.-B. Wang, *Dalton Trans.*, 2019, **48**, 13353-13359.
- 2 Y.-K. Huang, Z.-Y. Yang, S.-J. Yang and Y.-L. Xu, *J. Adv. Nanomater.*, 2017, **2**, 146-152.
- 3 X.-Y. Huang and X. Liu, *Appl. Surf. Sci.*, 2020, **505**, 144527.
- 4 X.-X. Qi, J.-H. Lv, K. Yu, H. Zhang, Z.-H. Su, L. Wang, C.-M. Wang and B.-B. Zhou, *RSC Adv.*, 2016, **6**, 72544-72550.
- 5 C.-L. Teng, H.-X. Xiao, Q. Cai, J.-T. Tang, T.-J. Cai and Q. Deng, *J. Coord. Chem.*, 2016, **69**, 2148-2163.
- 6 L.-W. Han, J.-X. Lin, Q. Yin, B. Karadeniz, H.-F. Li and R. Cao, *Cryst. Growth Des.*, 2016, **16**, 1213-1217.
- 7 X.-J. Dui, X.-Y. Wu, T. Teng, L. Zhang, H.-F. Chen, W.-B. Yang and C.-Z. Lu, *Inorg. Chem. Commun.*, 2015, **55**, 108-111.
- 8 R. Khoshnavazi, S. Fereydouni and L. Bahrami, *Water Sci. Technol.*, 2016, **73**, 1746-1755.
- 9 Y.-Y. Liu, J.-D. An, T.-T. Wang, Y. Li and B. Ding, *Inorg. Nano-Met. Chem.*, 2021, **51**, 976-984.
- 10 K.-X. Li, Y. Zhong, S.-L. Luo and W.-Y. Deng, *Appl. Cataly. B: Environ.*, 2020, **278**, 119313.
- 11 Z.-F. Zhao, B.-W. Cong, Z.-H. Su and B.-R. Li, *Cryst. Growth Des.*, 2020, **20**, 2753-2760.